Report

Neuron

Hippocampal Place Cells Couple to Three Different Gamma Oscillations during Place Field Traversal

Highlights

- Three distinct gamma oscillations are differently modulated by theta oscillation
- During theta phase precession, CA1 place cells couple to all gamma oscillations
- Some cells couple to various gamma oscillations during single place field traversal
- Individual cells integrate information from multiple gamma networks

Authors

Bálint Lasztóczi, Thomas Klausberger

Correspondence

balint.lasztoczi@meduniwien.ac.at (B.L.), thomas.klausberger@meduniwien.ac.at (T.K.)

In Brief

Lasztóczi and Klausberger show that firing of hippocampal place cells is coupled to three distinct gamma oscillations. Subsets of place cells couple to multiple gamma oscillations even during single place field traversals, indicating instantaneous integration and updating from different input networks.

Lasztóczi & Klausberger, 2016, Neuron *91*, 34–40
July 6, 2016
http://dx.doi.org/10.1016/j.neuron.2016.05.036

CellPress

CellPress

Neuron
Report

Hippocampal Place Cells Couple to Three Different Gamma Oscillations during Place Field Traversal

Bálint Lasztóczi[1,*] and Thomas Klausberger[1,*]
[1]Department of Cognitive Neurobiology, Centre for Brain Research, Medical University of Vienna, Spitalgasse 4, Vienna 1090, Austria
*Correspondence: balint.lasztoczi@meduniwien.ac.at (B.L.), thomas.klausberger@meduniwien.ac.at (T.K.)
http://dx.doi.org/10.1016/j.neuron.2016.05.036

SUMMARY

Three distinct gamma oscillations, generated in different CA1 layers, occur at different phases of concurrent theta oscillation. In parallel, firing of place cells displays phase advancement over successive cycles of theta oscillations while an animal passes through the place field. Is the theta-phase-precessing output of place cells shaped by distinct gamma oscillations along different theta phases during place field traversal? We simultaneously recorded firing of place cells and three layer-specific gamma oscillations using current-source-density analysis of multi-site field potential measurements in mice. We show that spike timing of place cells can tune to all three gamma oscillations, but phase coupling to the mid-frequency gamma oscillation conveyed from the entorhinal cortex was restricted to leaving a place field. A subset of place cells coupled to two different gamma oscillations even during single-place field traversals. Thus, an individual CA1 place cell can combine and relay information from multiple gamma networks while the animal crosses the place field.

INTRODUCTION

The hippocampus is a brain structure that hosts neuronal networks for spatial navigation and episodic memory (Buzsáki and Moser, 2013). Many hippocampal pyramidal cells have spatial receptive fields (“place fields”) (Buzsáki and Moser, 2013; O’Keefe and Nadel, 1978), allowing their instantaneous firing rate distribution to represent the animal’s current location (Wilson and McNaughton, 1993). In successive cycles of theta oscillation (5–12 Hz), spikes of place cells phase-advance as the animal runs through the place field (“theta phase precession”) (Huxter et al., 2008; O’Keefe and Recce, 1993). From the perspective of hippocampal neuronal networks, phase precession is a manifestation of theta cycle delimited firing sequences for compressed and segmented forward representations of behavioral episodes (Dragoi and Buzsáki, 2006; Foster and Wilson, 2007; Geisler et al., 2010; Maurer and McNaughton, 2007; Sanders et al., 2015; Skaggs et al., 1996). Such internally driven hippocampal memory sequences indeed occur independently of external cues (Pastalkova et al., 2008; Villette et al., 2015; Wang et al., 2015). The first active neuronal assembly of each theta cycle, constituted by the last spikes of respective place fields, may represent the animal’s actual location, linking the upcoming, internally generated cell assembly sequences within the theta cycle to environmental cues (Sanders et al., 2015). This suggests that early and late spikes of theta cycles may be controlled by different networks.

Cycles of 25–150 Hz gamma oscillation, amplitude-modulated by theta cycles (Bragin et al., 1995; Canolty et al., 2006; Stumpf, 1965), parse and segregate successive neuronal assemblies (Harris et al., 2003; Lisman and Idiart, 1995; Lisman and Jensen, 2013). With local field potential recordings, Colgin et al. (2009) discovered that, in CA1, distinct gamma oscillations with different frequencies co-occur during theta oscillations. Using sophisticated source separation techniques, Schomburg et al. (2014) delineated three distinct gamma oscillations with different spectral compositions, spatial distributions, and theta phase preferences. Entorhinal and CA3 input networks give rise to mid-frequency and slow gamma oscillations, respectively, whereas fast gamma oscillations are generated by local CA1 networks of pyramidal cells and interneurons. Do these different gamma oscillations influence the output of CA1 place cells at all? If so, do distinct gamma oscillations modulate different CA1 place cells or may they converge onto individual place cells and control spike timing at different sectors of the place field and different phases of the theta cycle?

RESULTS

We trained head-restrained mice to perform unidirectional runs for a water reward in a virtual linear maze. To record and separate layer-specific hippocampal gamma oscillations (Colgin et al., 2009; Lasztóczi and Klausberger, 2014; Schomburg et al., 2014), we inserted a linear silicon probe (50 μm site spacing) into the dorsal CA1 area and calculated instantaneous current-source-density (CSD) from the local field potentials (LFPs) recorded across all layers (Figure S1; Lasztóczi and Klausberger, 2014). During theta oscillations, we observed three spatiotemporally distinct CSD gamma oscillations identical to those reported previously in freely moving rats (Schomburg et al., 2014; Figure 1; Figure S2; n = 17 recording sessions from 7 mice). Bouts of mid-frequency gamma oscillations

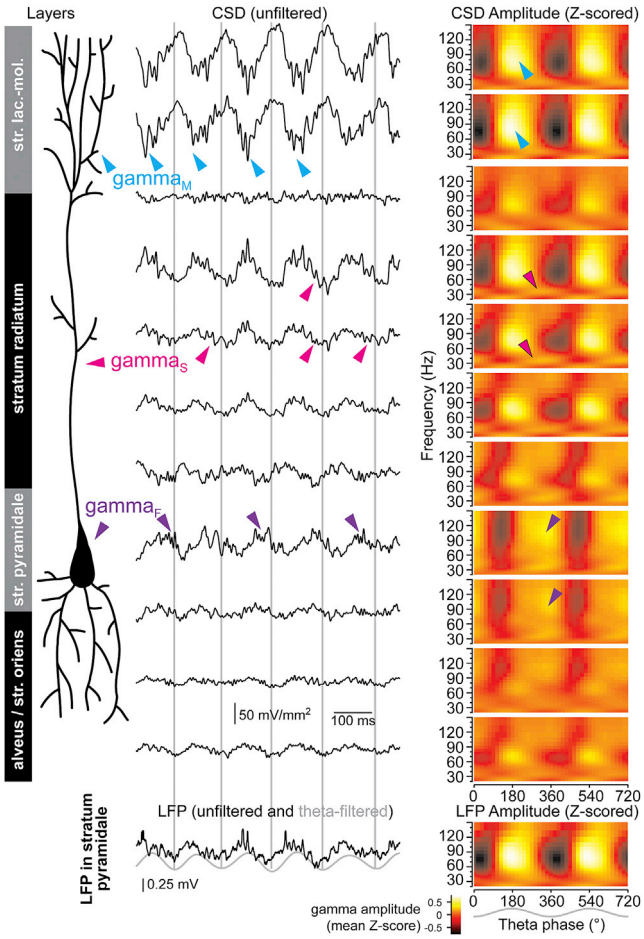

Figure 1. Three Gamma Oscillations in the CA1 Area of the Dorsal Hippocampus of Head-Fixed Awake Mice

Shown are CSD traces calculated for contacts located in different CA1 layers (indicated on the left). For comparison, the LFP recording from the pyramidal cell layer is also displayed (bottom). Right: modulation of gamma oscillation amplitude by theta phase (taken from the pyramidal cell layer LFP; 180° is peak). The color code represents the mean *Z*-scored wavelet amplitude of CSD (top plots, different layers) or LFP (bottom plot, pyramidal cell layer). Arrowheads mark mid-frequency ($gamma_M$, blue), slow ($gamma_S$, pink), and fast ($gamma_F$, purple) oscillations. $Gamma_M$ in the distal stratum radiatum, $gamma_S$ in the stratum pyramidale and stratum lacunosum-moleculare, and $gamma_F$ in the stratum oriens and stratum radiatum may represent return currents. Note the mixing of gamma oscillations in the LFP recorded in the stratum pyramidale.

See also Figure S2.

($gamma_M$, 57–86 Hz) occurred mostly on the peak (100°–290°) of theta oscillation and were dominant in the strata lacunosum moleculare and distal radiatum. Alternating with $gamma_M$, slow gamma oscillations ($gamma_S$, 32–41 Hz) occurred mostly on theta troughs (190°–400°) and were most distinct in the stratum radiatum. In turn, fast gamma oscillations ($gamma_F$, 92–133 Hz) were distributed around the stratum pyramidale and, similar to $gamma_S$, preferentially occurred on theta troughs (190°–400°). These three gamma oscillations have been shown to arise from layer-specific entorhinal ($gamma_M$), Schaffer collateral ($gamma_S$), and local GABAergic ($gamma_F$) synaptic inputs (Lasztóczi and Klausberger, 2014; Mizuseki et al., 2009; Schomburg et al., 2014). Different gamma oscillations appear less distinct in the LFP of the pyramidal cell layer (Figure 1).

In addition to the different gamma oscillations, we recorded neuronal spiking activity from the pyramidal cell layer of dorsal CA1. To avoid spurious coupling between spikes and the CSD arising from the slow components of action potential waveforms (Schomburg et al., 2012), we recorded action potentials with a separate silicon probe positioned 100–300 μm away from the linear probe (Figure S1). During traversal through a place field, the firing of 56 place cells (12 sessions, 6 mice) precessed to earlier phases in consecutive cycles of theta oscillation (Chen et al., 2013; Harvey et al., 2009; Ravassard et al., 2013). Thus, co-occurrence of a place cell's spikes with the three distinctly theta-modulated gamma oscillations depended on the animal's position within the place field. Coincidence of $gamma_M$ and spikes was maximal just before the animal left the place field, whereas $gamma_S$ and $gamma_F$ were strong during spikes throughout the traversal, particularly at the center of the place field (Figure 2; Figures S2 and S3).

Next, we tested whether this temporal coincidence was associated with coupling of place cells' spikes to the phase of different gamma oscillations. Measured over the entire place field and recording session, most place cells coupled to at least one type of gamma oscillation, and, for subsets of cells, a significant coupling to two or all three gamma oscillations could be demonstrated (Figure 3C). Spikes of individual place cells showed phase coupling to various combinations of distinct gamma oscillations variably depending on the position of the mouse within the place field. On average, phase coupling to $gamma_S$ and $gamma_F$ occurred throughout the place field with similar coupling strength (Figure 3; Figure S3; $\chi^2_{(2,104)} = 2.74$ and $\chi^2_{(2,56)} = 0.42$; n = 35 and 19; p = 0.25 and 0.89 for $gamma_S$ and $gamma_F$ r values, respectively; Friedman's test). In contrast, phase coupling to $gamma_M$ was curiously absent as the animal entered the place field but was observed in 18% of place cells just before the animal left the place field. The phase coupling strength of spikes to $gamma_M$ showed a significant increase with the animal's movement through the place field (Figure 3; Figure S3; $\chi^2_{(2,35)} = 20.67$; n = 12; $p = 3.3 \times 10^{-5}$; Friedman's test). Phase coupling to $gamma_M$, $gamma_S$, and $gamma_F$ was also observed for the firing of place cells with no phase precession (n = 15; Figure S3).

Combining data from multiple trials for analysis may disguise substantial and systematic variations in coupling to gamma oscillations during individual place field traversals (Cabral et al., 2014; Schmidt et al., 2009). Different gamma oscillations—including $gamma_M$ and $gamma_S$—often occurred within the same place field traversal and even within the same theta cycle (Figure 4; Figure S4). We tested whether coupling to multiple CSD gamma oscillations may occur within single runs or may be segregated over different trials (Bieri et al., 2014). To address this, one must overcome the problem of small numbers of spikes during a single place field traversal. For a particular gamma oscillation, we determined whether individual spikes occurred in the half of the gamma cycle surrounding the mean gamma phase of that particular place cell ("phase preference range") and determined the proportion of spikes within this phase range in

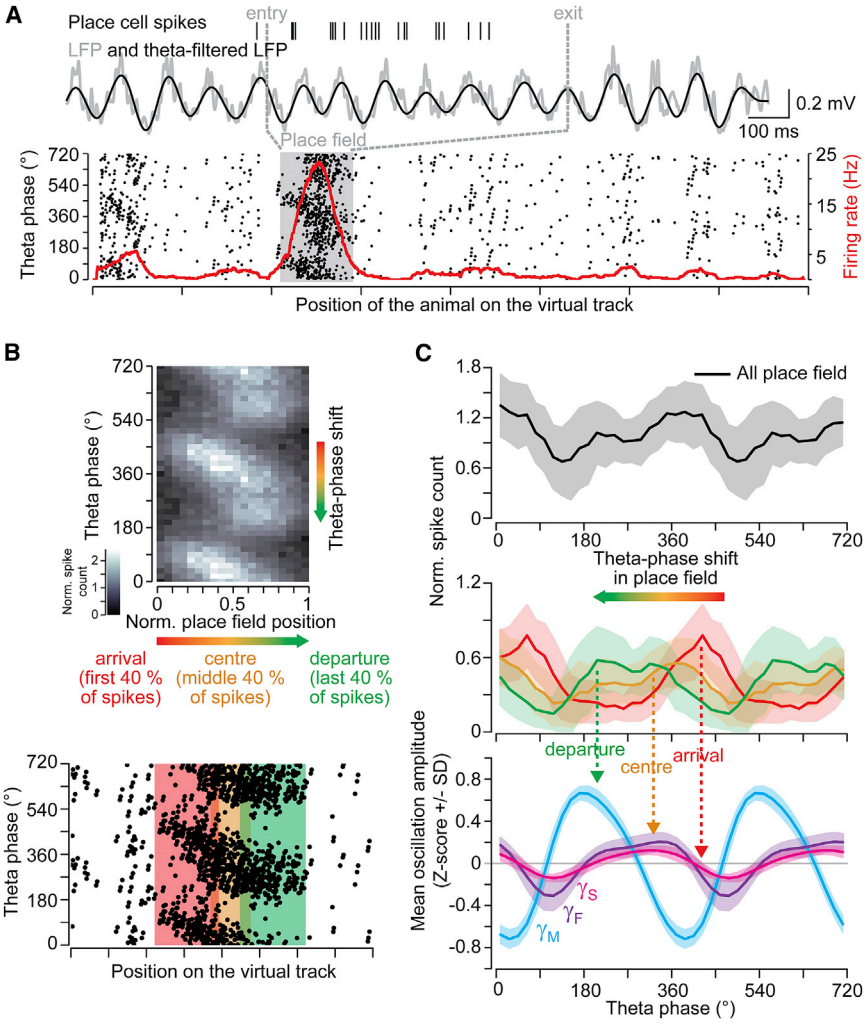

Figure 2. Co-occurrence of Place Cell Spikes and Different Gamma Oscillations Is Modulated by Theta Phase Precession

(A) Firing of a place cell during a single place field traversal (ticks, top) and during all trials of a recording session (dots, bottom). Concurrent LFP theta oscillations (top, trace from the pyramidal cell layer) and recorded theta phase values (bottom, left ordinate; data are duplicated to represent two theta cycles) are displayed. Note the phase precession of spikes within the place field.

(B) Theta phase versus position plot of spike density for all place cells (n = 56, top) and of spikes in an individual place field (bottom). The first, middle, and last 40% of spikes during place field traversal define arrival (red), center (orange), and departure (green) sectors.

(C) Theta phase histograms (mean ± SD, n = 56 place cells) of normalized spike counts within the entire place field (black, top) and in arrival, center, and departure sectors of the place fields (middle) and theta phase histograms of the amplitudes of $gamma_M$ (blue), $gamma_S$ (pink), and $gamma_F$ (purple) oscillations (bottom, n = 17 recording sessions from 7 mice).

See also Figure S2.

single place field traversals (Figures 4B–4D; Experimental Procedures). This yielded a number that represented the phase coupling tendencies toward one gamma oscillation for a single trial. We explored whether coupling tendencies to two distinct gamma oscillations co-occurred during individual place field traversals by comparing "proportions in preference range" values for pairs of distinct gamma oscillations in individual trials (Figures 4E and 4F). We found that increased proportions in preference range occurred within the same place field traversal for pairs of different gamma oscillations. The proportions in preference range for the two gamma oscillations were not correlated (Pearson's correlation, r = −0.013, p = 0.9, n = 98 runs for $gamma_M$/$gamma_S$ pairs; r = 0.057, p = 0.5, n = 140 runs for $gamma_F$/$gamma_S$ pairs; see also Table S1), indicating that, during individual place field traversals, place cells can couple to various gamma oscillations generated by distinct inputs and networks.

DISCUSSION

Our data directly link theta phase precession of CA1 place cells to the differential theta phase modulations of three distinct gamma oscillations, suggesting that theta rhythmic alternation of different gamma oscillations provides a temporal framework that supports flexible hippocampal information processing. Our finding that spikes of an individual place cell can phase-couple to multiple gamma oscillations of distinct network origin suggests that information processing in the hippocampus involves convergence of multiple networks on single pyramidal cells. Moreover, two gamma oscillations can both modulate the timing of spikes that occur within a single place field traversal (Figure 4). Thus, a single cell may combine information from multiple networks in a sub-second time frame, relevant for both navigation and episodic memory (Buzsáki and Moser, 2013).

Field potential oscillations in the gamma frequency range have been implicated in information transfer between synaptically connected brain areas (Fries, 2009). More recently sub-bands of gamma oscillations within the CA1 area of the dorsal hippocampus have been discovered to provide a mechanism for dynamic and selective communication from multiple converging input networks to the CA1 area of the hippocampus (Cabral et al., 2014; Colgin et al., 2009; Lasztóczi and Klausberger, 2014; Scheffer-Teixeira et al., 2012; Schomburg et al., 2014). In LFP recordings from the pyramidal cell layer of rat CA1, Colgin et al. (2009) defined "fast" and "slow" gamma oscillation on a spectral basis and linked these to entorhinal and CA3 pathways. Based on source separation by independent component analysis from multi-layer recordings, Schomburg et al. (2014) could identify slow, mid-frequency, and fast gamma oscillations, which are generated in different layers of CA1. Similar to this latter

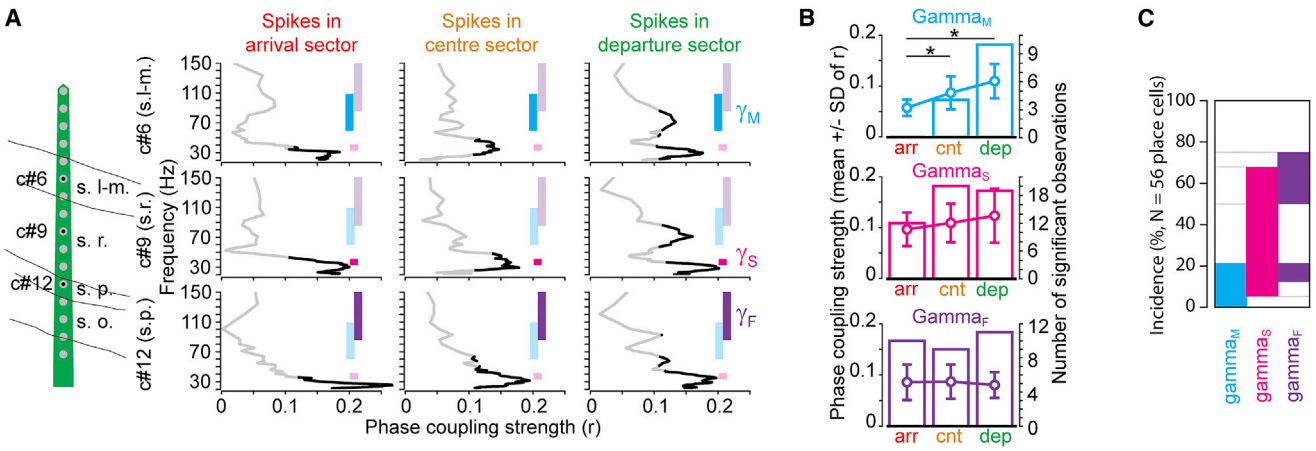

Figure 3. Phase Coupling of Place Cells' Spikes to Three Distinct Gamma Oscillations and Their Dependence on the Animal's Position within the Place Field

(A) Left: schematic of the recording sites. Right: spectral analysis of coupling strength for spikes of an individual place cell in arrival, center, and departure sectors (columns) to CSD gamma oscillations from three contacts in different layers (rows; black indicates significant coupling, $\alpha = 0.05$, Rayleigh test, n = 277 spikes/sector). Color-coded bars indicate the frequency ranges for different gamma oscillations, highlighted in the relevant layer. Note a sector dependence of coupling to $gamma_M$ (top row).

(B) Incidence (bars, n = 56 place cells) and strength (circles; mean ± SD of r; n = 12, 35, and 19 place cells for $gamma_M$, $gamma_S$, and $gamma_F$, respectively) of phase coupling of place cells' spikes to distinct gamma oscillations in arrival, center, and departure sectors of the place field (*$p < 0.05$, Dunn's post hoc and Friedman's test).

(C) Occurrence and co-incidence of significant phase coupling to different gamma oscillations.

See also Figure S3.

study, we used multiple-site silicon probe recordings and CSD analysis to suppress volume-conducted signal components and to localize dynamic current sources and sinks of different gamma oscillations (Einevoll et al., 2013; Nicholson and Freeman, 1975). We established three layer-specific gamma oscillations in the dorsal CA1 of head-fixed awake mice (Figure 1), with spectral, temporal (theta phase), and laminar distributions similar to those reported by Schomburg et al. (2014) in freely moving rats, and conclude that they correspond to gamma oscillations conveyed by extrahippocampal (entorhinal, $gamma_M$) and intrahippocampal (CA3, $gamma_S$) input pathways and high-frequency gamma oscillations generated by a local network of CA1 interneurons and pyramidal cells ($gamma_F$).

In recent reports, place field traversals (Bieri et al., 2014) and theta sequences (Zheng et al., 2016) of different content (encoding or recall) were shown to be segregated into extended epochs with slow and fast gamma oscillations. However, in accordance with our data, a substantial proportion of theta cycles (Colgin et al., 2009), place field traversals (Bieri et al., 2014), and theta sequences (Zheng et al., 2016) are associated with co-occurrence of oscillations at different gamma frequency ranges. By employing source separation in multi-layer recordings, we show that phase coupling to multiple gamma oscillations (e.g., $gamma_M$ and $gamma_S$) occurs within a single place field traversal on a sub-second time scale (Figure 4). In addition, we observed a characteristic position dependence of coincidence between spikes and distinct gamma oscillations (particularly $gamma_M$) emerging from theta phase precession of place cells (O'Keefe and Recce, 1993) and differential theta phase modulation of gamma oscillations (Figure 2). Surprisingly, upon entering the place field, when place cells fire on the ascending phase of theta cycles, little coincidence and no phase coupling to $gamma_M$ were observed, suggesting little if any influence of entorhinal afferents. In a subset of place cells, however, phase coupling to $gamma_M$ occurred just before the animal left the cell's place field (Figure 3). These spikes occurred around the peak of theta oscillation, when excitation of distal dendrites of CA1 pyramidal cells by layer 3 cells of the medial entorhinal cortex is maximal (Mizuseki et al., 2009). This transient $gamma_M$ synchronization may allow extrahippocampal inputs, carrying representations of environmental cues and possibly inducing plasticity (Bittner et al., 2015; Brun et al., 2008; Schlesiger et al., 2015; Takahashi and Magee, 2009), to control the active cell assemblies. Although the complex relationship between phase precession and firing sequences is not completely understood (Aghajan et al., 2015; Feng et al., 2015; Foster and Wilson, 2007), anchored firing fields with phase precession and stable phase offset (Chen et al., 2013; Harvey et al., 2009; Ravassard et al., 2013) are consistent with the expression of time-compressed theta firing sequences (Dragoi and Buzsáki, 2006; Feng et al., 2015; Geisler et al., 2010; Skaggs et al., 1996). In the context of network models of phase precession (Geisler et al., 2010; Sanders et al., 2015; Skaggs et al., 1996), $gamma_M$ may coordinate the initiation of firing sequences (Figure 4G) and anchor place fields to the animals' current location (Cabral et al., 2014). $Gamma_S$ and $gamma_F$, in turn, coordinate spike timing later in the theta cycle (earlier in the place field), where spikes represent "mind travel" to upcoming positions (Sanders et al., 2015) and may occur as part of internally generated memory sequences (Pastalkova et al., 2008; Villette et al., 2015; Wang et al., 2015) retrieved from associative CA3 and CA1 gamma networks (Figure 4G). Indeed, the balance of different gamma oscillations is modulated by behavioral demand

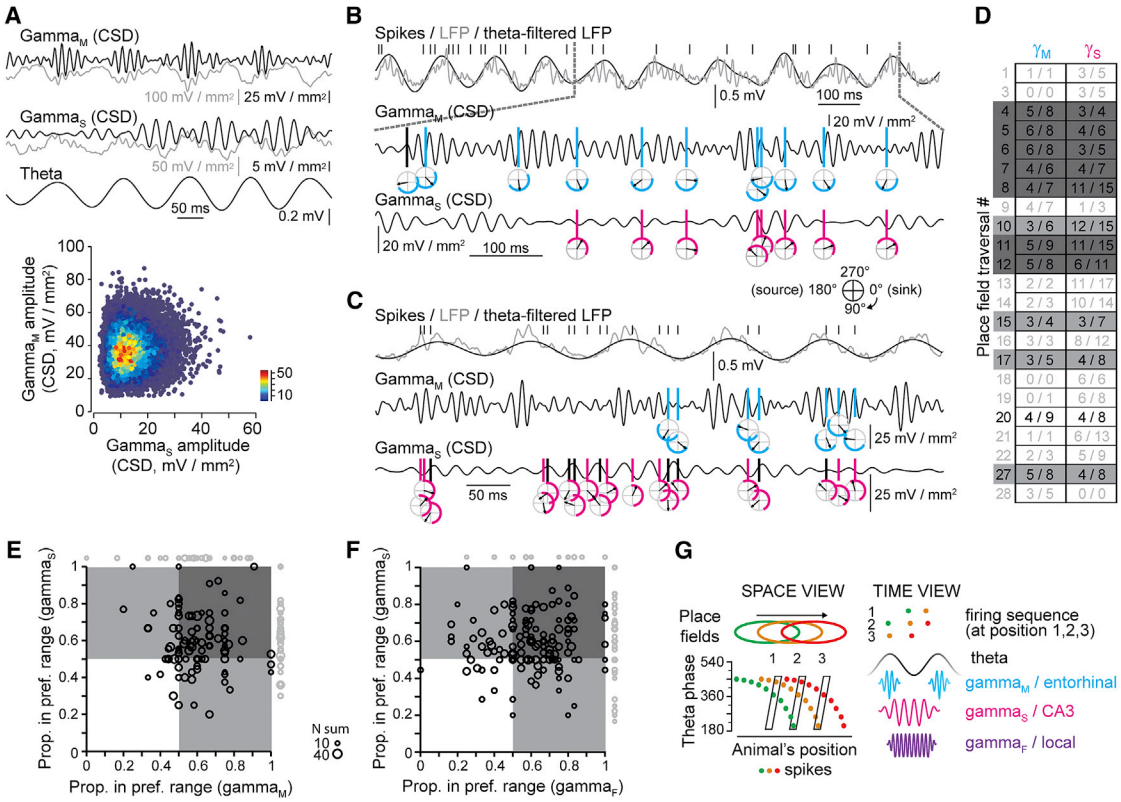

Figure 4. The Firing of Place Cells Can Couple to Two Different Gamma Oscillations during a Single Place Field traversal

(A) CSD traces of gamma$_M$ and gamma$_S$ (from the stratum lacunosum-moleculare and stratum radiatum, filtered for the gamma$_M$ and gamma$_S$ frequency range, respectively; gray, raw CSD traces) and theta oscillations (LFP) from the stratum pyramidale. Bottom: amplitudes of gamma$_M$ versus gamma$_S$ plotted for all theta cycles in one experiment (the color scale indicates the number of points/bin). Note the occurrence of strong gamma$_M$ and gamma$_S$ within the same theta cycle.

(B) Spikes of a place cell (ticks) during a single place field traversal and theta oscillations recorded from the pyramidal cell layer. Below, spikes and CSD traces for gamma$_M$ and gamma$_S$ are plotted for sectors with significant coupling (center and departure for gamma$_M$ and departure for gamma$_S$). The circular diagram below each spike indicates the instantaneous CSD gamma phase of the spike. Spikes within the preference range (the half of the gamma cycle surrounding the mean firing phase of the cell) are colored.

(C) Same as in (B) for a different place cell.

(D) For a single place cell, the proportions of spikes within the preference range for gamma$_M$ and gamma$_S$ are indicated for individual place field traversals. Only spikes in sectors with significant coupling were considered. Traversals with more spikes occurring in the preference range for both (dark gray, note prevalence), one (light gray), or neither (white) gamma oscillations are indicated. Traversals with less than four spikes for either gamma oscillation are not evaluated (shown in gray).

(E) Proportions of spikes within the preference range for gamma$_M$ (abscissa) and gamma$_S$ (ordinate) are plotted for individual place field traversals. Circle size represents the sum of the number of spikes included for the two oscillations. Traversals with less than four spikes for one or both gamma oscillation are plotted in gray or omitted, respectively. n = 178 traversals, 5 cells, 5 mice. Most traversals have an increased proportion of spikes within the preferred phase of both gamma oscillations (dark gray).

(F) Same as in (E) for gamma$_F$ and gamma$_S$. n = 227 traversals, 6 cells, 3 experiments, 2 mice. Because of conservative inclusion criteria (Supplemental Experimental Procedures), no gamma$_M$/gamma$_F$ oscillation pair could be analyzed.

(G) Schematic of the relationship between different gamma oscillations, theta phase precession in place cells, and firing sequences of place cells. Place cells can couple to different gamma oscillations during a place field traversal. Note that, when the animal is in position 2 and leaving the green place field (space view), the green place cell fires first in the theta cycle and is coupled to gamma$_M$ originating from the entorhinal cortex (time view).

See also Figure S4 and Table S1.

(Cabral et al., 2014). Our data suggest that spatial selectivity and theta phase precession in CA1 pyramidal cells are structured by rapid, concerted dynamics imposed by converging entorhinal, CA3, and local gamma oscillatory networks.

EXPERIMENTAL PROCEDURES

Animals, Surgery, and Virtual Maze

All animal procedures were carried out under licenses approved by the Austrian Ministry of Science and in accordance with the relevant regulations of the Medical University of Vienna. Adult male C57BL/6 mice (weighing around 30 g) were implanted with a plastic head plate, habituated to head restraint, and trained to perform unidirectional runs on an air-supported Styrofoam ball in a virtual linear maze (Phenosys) for a small water reward (Figure S1).

In Vivo Electrophysiology

Before recordings, mice were anesthetized, and a cranial window was drilled above the right dorsal hippocampus. On each recording day, the animals were head-restrained and mounted onto the jet ball without anesthesia, the brain surface was washed with saline, and the recording electrodes were stereotactically inserted. LFP was recorded from multiple sites across the CA1 layers

with a linear silicon probe (single shank, 16-site, 50 μm spacing; Neuronexus). Action potentials were recorded using a separate multi-shank silicon probe (16 clustered recording sites) 100–300 μm away from the linear probe in the pyramidal layer of the CA1 region (gamma oscillations are coherent within the same layer over hundreds of micrometers; Schomburg et al., 2014). Only recordings with evidence obtained for the localization of electrodes in the desired position were included in this study. Of 514 recorded and isolated units with >300 spikes during theta oscillations, 146 units were spatially modulated (the firing rate at any position exceeded 3× mean firing rate). Cells with incomplete place fields on either end of the track or insufficient spikes within the place field (<250) were discarded, resulting in 69 units with at least one place field. This includes 55 units (with 56 place fields) with phase precession (circular-linear correlation $r > 0.24$) and 14 units (with 15 place fields) with no phase precession. For simplicity, we refer to these as 56 and 15 place cells with and without phase precession, respectively, throughout the manuscript.

Data Analysis

CSD traces were directly derived from the LFP recordings of the linear silicon probe as the second spatial derivative (Lasztóczi and Klausberger, 2014). The instantaneous theta phase was determined by linear interpolation between peaks (180°) and troughs (0° and 360°) of the theta-filtered (5–12 Hz) LFP signal recorded from the stratum oriens (equivalent to the pyramidal layer). To analyze gamma oscillations, CSD traces were subjected to wavelet transformation (Lasztóczi and Klausberger, 2014) with a complex Morlet wavelet (20–150 Hz, 52 logarithmically equidistant frequencies, wavelet parameters of 1 and 1.5; we designated 0° and 360° as the maximum sink and 180° as the maximum source).

Seeking a compromise between a good spatial resolution and a sufficient number of spikes to carry out phase coupling analyses, we defined three spatial sectors for each place field as the range containing the first (arrival sector), the middle (center sector), and the last (departure sector) 40% of all spikes within the place field. By assuring an equal number of spikes in all sectors, this allowed direct comparisons of the coupling strength (mean vector length, r) in the different sectors. Instantaneous wavelet transform spectra corresponding to spikes were summarized by place field sectors with phase coupling statistics calculated in a spectral manner. The uniformity of phase distribution was assessed by Rayleigh test ($\alpha = 0.05$) separately for each wavelet scale.

To analyze phase coupling in small samples of single place field traversals, for each trial and gamma oscillation, we determined the proportion of spikes within a ± 90° range from the mean phase (calculated over all traversals; sectors with significant coupling included) and used this as a proxy for the phase bias. In a subset of place cells, we observed significant phase bias by two different gamma oscillations during individual place field traversals and addressed their interactions by correlating the proportions within the preference range (see the Supplemental Experimental Procedures for another method of quantifying correlations).

Statistics

Data are displayed as mean ± SD. Spatial tendencies over the different sectors were tested with Friedman's test followed by Dunn's post hoc test. Distributions of single place field traversals proportions in preference range were compared by Kolmogorov-Smirnov test, and correlations were measured as Pearson's linear correlation.

See the Supplemental Experimental Procedures for further details.

SUPPLEMENTAL INFORMATION

Supplemental Information includes Supplemental Experimental Procedures, four figures, and one table and can be found with this article online at http://dx.doi.org/10.1016/j.neuron.2016.05.036.

AUTHOR CONTRIBUTIONS

B.L. and T.K. designed the study, conducted the experiments, analyzed the data, and wrote the manuscript.

ACKNOWLEDGMENTS

We thank Romana Hauer and Erzsébet Borók for excellent technical assistance, Hugo Malagon-Viña for help with programing, Thomas Forro for help with illustrations, and members of the T.K. lab for discussions. We thank Peter Somogyi for commenting on an earlier version of the manuscript. This work was supported in part by the SCIC03 grant of the Vienna Science and Technology Fund.

Received: February 1, 2016
Revised: April 13, 2016
Accepted: May 16, 2016
Published: July 6, 2016

REFERENCES

Aghajan, Z.M., Acharya, L., Moore, J.J., Cushman, J.D., Vuong, C., and Mehta, M.R. (2015). Impaired spatial selectivity and intact phase precession in two-dimensional virtual reality. Nat. Neurosci. *18*, 121–128.

Bieri, K.W., Bobbitt, K.N., and Colgin, L.L. (2014). Slow and fast γ rhythms coordinate different spatial coding modes in hippocampal place cells. Neuron *82*, 670–681.

Bittner, K.C., Grienberger, C., Vaidya, S.P., Milstein, A.D., Macklin, J.J., Suh, J., Tonegawa, S., and Magee, J.C. (2015). Conjunctive input processing drives feature selectivity in hippocampal CA1 neurons. Nat. Neurosci. *18*, 1133–1142.

Bragin, A., Jandó, G., Nádasdy, Z., Hetke, J., Wise, K., and Buzsáki, G. (1995). Gamma (40-100 Hz) oscillation in the hippocampus of the behaving rat. J. Neurosci. *15*, 47–60.

Brun, V.H., Leutgeb, S., Wu, H.Q., Schwarcz, R., Witter, M.P., Moser, E.I., and Moser, M.B. (2008). Impaired spatial representation in CA1 after lesion of direct input from entorhinal cortex. Neuron *57*, 290–302.

Buzsáki, G., and Moser, E.I. (2013). Memory, navigation and theta rhythm in the hippocampal-entorhinal system. Nat. Neurosci. *16*, 130–138.

Cabral, H.O., Vinck, M., Fouquet, C., Pennartz, C.M., Rondi-Reig, L., and Battaglia, F.P. (2014). Oscillatory dynamics and place field maps reflect hippocampal ensemble processing of sequence and place memory under NMDA receptor control. Neuron *81*, 402–415.

Canolty, R.T., Edwards, E., Dalal, S.S., Soltani, M., Nagarajan, S.S., Kirsch, H.E., Berger, M.S., Barbaro, N.M., and Knight, R.T. (2006). High gamma power is phase-locked to theta oscillations in human neocortex. Science *313*, 1626–1628.

Chen, G., King, J.A., Burgess, N., and O'Keefe, J. (2013). How vision and movement combine in the hippocampal place code. Proc. Natl. Acad. Sci. USA *110*, 378–383.

Colgin, L.L., Denninger, T., Fyhn, M., Hafting, T., Bonnevie, T., Jensen, O., Moser, M.B., and Moser, E.I. (2009). Frequency of gamma oscillations routes flow of information in the hippocampus. Nature *462*, 353–357.

Dragoi, G., and Buzsáki, G. (2006). Temporal encoding of place sequences by hippocampal cell assemblies. Neuron *50*, 145–157.

Einevoll, G.T., Kayser, C., Logothetis, N.K., and Panzeri, S. (2013). Modelling and analysis of local field potentials for studying the function of cortical circuits. Nat. Rev. Neurosci. *14*, 770–785.

Feng, T., Silva, D., and Foster, D.J. (2015). Dissociation between the experience-dependent development of hippocampal theta sequences and single-trial phase precession. J. Neurosci. *35*, 4890–4902.

Foster, D.J., and Wilson, M.A. (2007). Hippocampal theta sequences. Hippocampus *17*, 1093–1099.

Fries, P. (2009). Neuronal gamma-band synchronization as a fundamental process in cortical computation. Annu. Rev. Neurosci. *32*, 209–224.

Geisler, C., Diba, K., Pastalkova, E., Mizuseki, K., Royer, S., and Buzsáki, G. (2010). Temporal delays among place cells determine the frequency of population theta oscillations in the hippocampus. Proc. Natl. Acad. Sci. USA *107*, 7957–7962.

Harris, K.D., Csicsvari, J., Hirase, H., Dragoi, G., and Buzsáki, G. (2003). Organization of cell assemblies in the hippocampus. Nature *424*, 552–556.

Harvey, C.D., Collman, F., Dombeck, D.A., and Tank, D.W. (2009). Intracellular dynamics of hippocampal place cells during virtual navigation. Nature *461*, 941–946.

Huxter, J.R., Senior, T.J., Allen, K., and Csicsvari, J. (2008). Theta phase-specific codes for two-dimensional position, trajectory and heading in the hippocampus. Nat. Neurosci. *11*, 587–594.

Lasztóczi, B., and Klausberger, T. (2014). Layer-specific GABAergic control of distinct gamma oscillations in the CA1 hippocampus. Neuron *81*, 1126–1139.

Lisman, J.E., and Idiart, M.A.P. (1995). Storage of 7 +/- 2 short-term memories in oscillatory subcycles. Science *267*, 1512–1515.

Lisman, J.E., and Jensen, O. (2013). The θ-γ neural code. Neuron *77*, 1002–1016.

Maurer, A.P., and McNaughton, B.L. (2007). Network and intrinsic cellular mechanisms underlying theta phase precession of hippocampal neurons. Trends Neurosci. *30*, 325–333.

Mizuseki, K., Sirota, A., Pastalkova, E., and Buzsáki, G. (2009). Theta oscillations provide temporal windows for local circuit computation in the entorhinal-hippocampal loop. Neuron *64*, 267–280.

Nicholson, C., and Freeman, J.A. (1975). Theory of current source-density analysis and determination of conductivity tensor for anuran cerebellum. J. Neurophysiol. *38*, 356–368.

O'Keefe, J., and Nadel, L. (1978). The Hippocampus as a Cognitive Map (Clarendon).

O'Keefe, J., and Recce, M.L. (1993). Phase relationship between hippocampal place units and the EEG theta rhythm. Hippocampus *3*, 317–330.

Pastalkova, E., Itskov, V., Amarasingham, A., and Buzsáki, G. (2008). Internally generated cell assembly sequences in the rat hippocampus. Science *321*, 1322–1327.

Ravassard, P., Kees, A., Willers, B., Ho, D., Aharoni, D., Cushman, J., Aghajan, Z.M., and Mehta, M.R. (2013). Multisensory control of hippocampal spatiotemporal selectivity. Science *340*, 1342–1346.

Sanders, H., Rennó-Costa, C., Idiart, M., and Lisman, J. (2015). Grid Cells and Place Cells: An Integrated View of their Navigational and Memory Function. Trends Neurosci. *38*, 763–775.

Scheffer-Teixeira, R., Belchior, H., Caixeta, F.V., Souza, B.C., Ribeiro, S., and Tort, A.B. (2012). Theta phase modulates multiple layer-specific oscillations in the CA1 region. Cereb. Cortex *22*, 2404–2414.

Schlesiger, M.I., Cannova, C.C., Boublil, B.L., Hales, J.B., Mankin, E.A., Brandon, M.P., Leutgeb, J.K., Leibold, C., and Leutgeb, S. (2015). The medial entorhinal cortex is necessary for temporal organization of hippocampal neuronal activity. Nat. Neurosci. *18*, 1123–1132.

Schmidt, R., Diba, K., Leibold, C., Schmitz, D., Buzsáki, G., and Kempter, R. (2009). Single-trial phase precession in the hippocampus. J. Neurosci. *29*, 13232–13241.

Schomburg, E.W., Anastassiou, C.A., Buzsáki, G., and Koch, C. (2012). The spiking component of oscillatory extracellular potentials in the rat hippocampus. J. Neurosci. *32*, 11798–11811.

Schomburg, E.W., Fernández-Ruiz, A., Mizuseki, K., Berényi, A., Anastassiou, C.A., Koch, C., and Buzsáki, G. (2014). Theta phase segregation of input-specific gamma patterns in entorhinal-hippocampal networks. Neuron *84*, 470–485.

Skaggs, W.E., McNaughton, B.L., Wilson, M.A., and Barnes, C.A. (1996). Theta phase precession in hippocampal neuronal populations and the compression of temporal sequences. Hippocampus *6*, 149–172.

Stumpf, C. (1965). The Fast Component in the Electrical Activity of Rabbit's Hippocampus. Electroencephalogr. Clin. Neurophysiol. *18*, 477–486.

Takahashi, H., and Magee, J.C. (2009). Pathway interactions and synaptic plasticity in the dendritic tuft regions of CA1 pyramidal neurons. Neuron *62*, 102–111.

Villette, V., Malvache, A., Tressard, T., Dupuy, N., and Cossart, R. (2015). Internally Recurring Hippocampal Sequences as a Population Template of Spatiotemporal Information. Neuron *88*, 357–366.

Wang, Y., Romani, S., Lustig, B., Leonardo, A., and Pastalkova, E. (2015). Theta sequences are essential for internally generated hippocampal firing fields. Nat. Neurosci. *18*, 282–288.

Wilson, M.A., and McNaughton, B.L. (1993). Dynamics of the hippocampal ensemble code for space. Science *261*, 1055–1058.

Zheng, C., Bieri, K.W., Hsiao, Y.T., and Colgin, L.L. (2016). Spatial Sequence Coding Differs during Slow and Fast Gamma Rhythms in the Hippocampus. Neuron *89*, 398–408.